Pure appl. geophys. 166 (2009) 259–281
0033–4553/09/010259–23
DOI 10.1007/s00024-008-0431-8

Pure and Applied Geophysics

Reconstruction of Tsunami Inland Propagation on December 26, 2004 in Banda Aceh, Indonesia, through Field Investigations

Franck Lavigne,[1] Raphaël Paris,[2] Delphine Grancher,[1] Patrick Wassmer,[1] Daniel Brunstein,[1] Franck Vautier,[2] Frédéric Leone,[3] François Flohic,[4] Benjamin De Coster,[4] Taufik Gunawan,[5] Christopher Gomez,[1] Anggri Setiawan,[6] Rino Cahyadi,[6] and Fachrizal[5]

Abstract—This paper presents the results from an extensive field data collection effort following the December 26, 2004 earthquake and tsunami in Banda Aceh, Sumatra. The data were collected under the auspices of TSUNARISQUE, a joint French-Indonesian program dedicated to tsunami research and hazard mitigation, which has been active since before the 2004 event. In total, data from three months of field investigations are presented, which detail important aspects of the tsunami inundation dynamics in Banda Aceh. These include measurements of runup, tsunami wave heights, flow depths, flow directions, event chronology and building damage patterns. The result is a series of detailed inundation maps of the northern and western coasts of Sumatra including Banda Aceh and Lhok Nga.

Among the more important findings, we obtained consistent accounts that approximately ten separate waves affected the region after the earthquake; this indicates a high-frequency component of the tsunami wave energy in the extreme near-field. The largest tsunami wave heights were on the order of 35 m with a maximum runup height of 51 m. This value is the highest runup value measured in human history for a seismically generated tsunami. In addition, our field investigations show a significant discontinuity in the tsunami wave heights and flow depths along a line approximately 3 km inland, which the authors interpret to be the location of the collapse of the main tsunami bore caused by sudden energy dissipation. The propagating bore looked like a breaking wave from the landward side although it has distinct characteristics. Patterns of building damage are related to the location of the propagating bore with overall less damage to buildings beyond the line where the bore collapsed. This data set was built to be of use to the tsunami community for the purposes of calibrating and improving existing tsunami inundation models, especially in the analysis of extreme near-field events.

Key words: Tsunami, runup, tsunami bore, inundation, intensity scale, building damage.

[1] Laboratoire de Géographie Physique, UMR 8591 CNRS, 1 Place A. Briand, 92190 Meudon, France. E-mail: franck.lavigne@univ-paris1.fr

[2] Géolab UMR 6042 CNRS, Maison de la Recherche, 4 rue Ledru, 63057 Clermont-Ferrand, France.

[3] Department de Géographie, université Paul Valéry, Montpelliar, France.

[4] Planet Risk, 6 rue Marie-Thérèse, 91230 Montgeron, France.

[5] Badan Meteorologi dan Geofisika, Jl. Angkasa 1 No.2, Kemayoran, Jakarta Pusat, Indonesia.

[6] University Gadjah Mada (UGM), Jl Kaliurang, Yogyakarta, Indonesia.

1. Introduction

The 2004 Indian Ocean tsunami was triggered by a 9.15 magnitude earthquake (Meltzner *et al.*, 2006; Chlieh *et al.*, 2007) that occurred at 0:58:53 GMT, 7:58:53 LT (USGS) (t_{EQ}). The epicenter was located at 3.3 N, 95.8 E (Fig. 1) with a focal depth of approximately 30 km. The earthquake was responsible for a sudden fault slip estimated on average from 12–15 m (Synolakis *et al.*, 2005; Lay *et al.*, 2005) to 20 m (Fu and Sun, 2006). The seismic moment estimate (Mo = 1.3 5 × 10^{30} dyne-cm), based on the

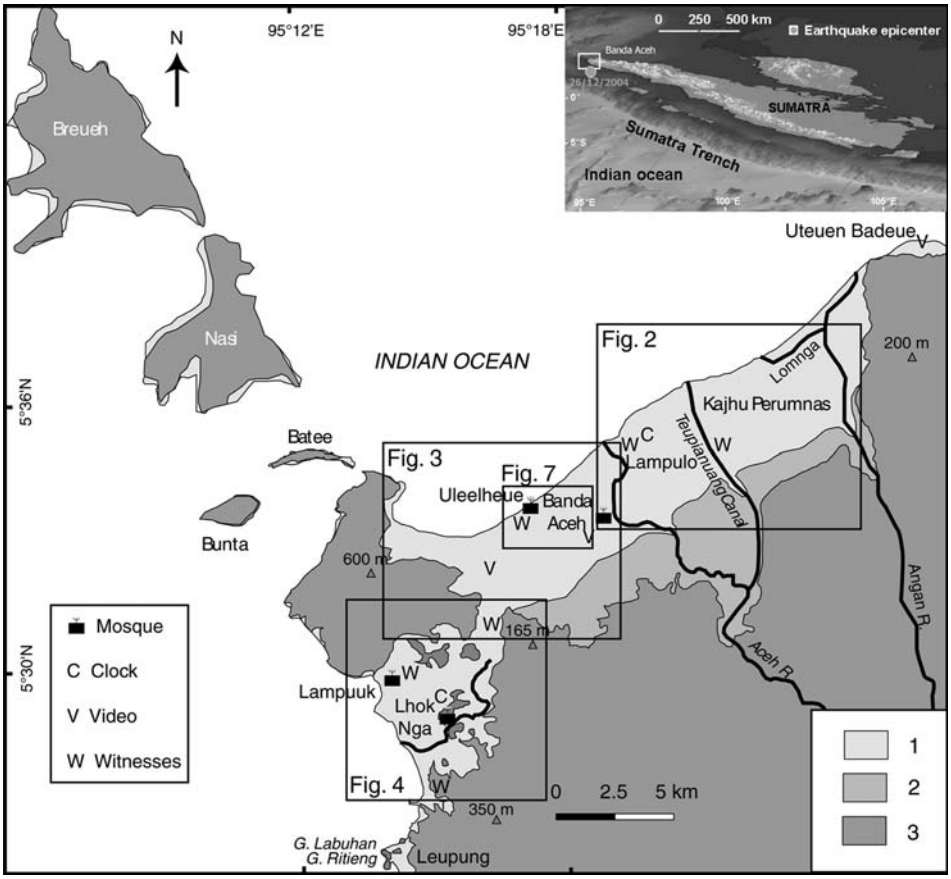

Figure 1

Locations of video recordings, recovered clocks, and reliable eyewitness observations. 1: Coastal plains flooded by the tsunami; 2: non-flooded coastal plains; 3: uplands. Insert 3D-map showing the Sumatra Island, the studied area, and the epicenter of the 26/12/2004 earthquake. The video taken at Uteuen Badeue, on the eastern edge of the Banda Aceh Bay, was recorded by the chief of the Fishery Regional Office from the top of a cliff. The movie that was shot near the Baiturrahman mosque in downtown Banda Aceh has been shown worldwide on TV. The one at Peukan Bada has been recorded during a wedding party. The last two movies were analyzed in detail in order to calculate the tsunami velocity (Fritz *et al.*, 2006).

measurement of split modes of free oscillations of the Earth, is about three times larger than the 4 5 $\times$ 10^{29} dyne-cm measured from traditional long-period surface waves (STEIN and OKAL, 2005). In the model suggested by CHLIEH *et al.* (2007), the latitudinal distribution of released moment has three distinct peaks at about 4° N, 7° N, and 9° N, which compares well to the latitudinal variations seen in the seismic inversion and of the analysis of radiated T waves. The earthquake-induced damage to buildings was rather limited in Banda Aceh City. Along the coastline, the damage to structures was difficult to assess because the tsunami had totally destroyed the buildings.

Since the 1980s and the 1990s, the development of numerical modeling has increased the knowledge of offshore tsunami propagation (e.g., SYNOLAKIS, 1987; IMAMURA and SHUTO, 1990; CARRIER *et al.*, 2003). Models currently in use include the French simulation code developed by the Commissariat à l'Energie Atomique (CEA) (HEINRICH *et al.*, 1998; HÉBERT *et al.*, 2001), the Method of Splitting Tsunami (MOST) model used by the Pacific Marine Environmental Laboratory of the National Oceanic and Atmospheric Administration (NOAA PMEL) (TITOV and SYNOLAKIS, 1998), the FUNWAVE model (developed by the Centre of Applied Coastal Research: KIRBY, 2003), and the code produced by workers from Japan called TUNAMI N2 (GOTO *et al.*, 1997). Most of these models use linear or nonlinear shallow water assumptions, with or without dispersive effects, to study tsunamis generated by earthquakes and submarine landslides. Such models provide accurate simulations of far-field propagation of the tsunami waves. Some models like MOST have also been extensively validated against runup signatures, even for extreme events like the Okushiri tsunami (> 30 m runup). However, other models have not yet been used extensively in simulating near-field propagation and detailed inland wave behavior (e.g., transient bore propagation). This fact can be partially explained by a lack of a highly accurate DEM and source model, however mainly by a lack of accurate field data necessary to calibrate the models. Therefore, few inundation maps have been drawn following a major tsunami, and tsunami hazard mapping based on numerical modeling is still limited, except along the Japanese coast and the West coast of the USA (TITOV *et al.*, 2004; WONG *et al.*, 2005).

The December 26th, 2004 Indian Ocean earthquake and tsunami offers an opportunity to enhance our knowledge on tsunami processes and modeling, both near-shore and on land. Several research teams involved in the study of this unusual event thus far have focused their efforts on the tsunami origin — i.e. the earthquake mechanism — and/or trans-oceanic propagation (AMMON *et al.*, 2005; GEIST *et al.*, 2007; HÉBERT *et al.*, 2007; ENGDAHL *et al.*, 2007; VALLÉE, 2007). A few weeks after the disaster, other research groups conducted reconnaissance surveys along the Indonesian coasts in the framework of the International Tsunami Survey Teams (ITST) headed by BORRERO (2005a,b), BORRERO *et al.* (2006), YALCINER *et al.* (2005), and TSUJI *et al.* (2006). Such rapid field surveys were very useful in the aftermath of this exceptional tsunami that inundated hundreds of square kilometers of coasts and destroyed thousands of houses. For example, BORRERO (2005b) provided a table of overland flow depths and direction from throughout Banda Aceh, as well as a detailed map of the inundation extents and the first descriptions

of the wave crossing from Lhok Nga to the southwestern parts of Banda Aceh. Such data were enough to do preliminary modelling. However, additional data are needed to conduct in-depth analysis at a local scale.

An extensive database of tsunami propagation evidence has been collected for the Banda Aceh and Lhok Nga districts (Fig. 1). The data were collected under the auspices of TSUNARISQUE, a joint French-Indonesian program dedicated to tsunami research and hazard mitigation, which has been active since before the 2004 event. At the time of the Indian Ocean tsunami disaster, authors 1 and 2 accompanied the second ITST from 19 to 29 January 2005, and supplemented this preliminary survey by six subsequent trips conducted between August 2005 and August 2006. Finally, this program was completed after three months of field investigations, and with the help of more than 30 researchers, technicians, and students.

In this paper we synthesized the main data collected during these field trips in order to provide the most complete and accurate reconstruction of the dynamics of the tsunami inundation as possible. This analysis includes various aspects of the phenomenon, such as the time and space evolution of the different waves, tsunami height and runup variations, flow-depth distribution, as well as the contribution of backwash to coastal erosion. In addition, these parameters were discussed with several additional parameters, such as topography, location of tsunami bores, and building damages. Complementary analyses of the 2004 tsunami deposits and observations on the geomorphological effects of the tsunami were previously published (Paris *et al*., 2007a, b). Beyond the direct contribution of this work to the understanding of the effects of giant tsunami waves on coastal areas, our database offers an opportunity to test, calibrate, and improve the existing numerical simulation codes, which are fundamental in assessing the hazards of future events. In this respect, a high-resolution DEM has been built from various datasets collected during the campaigns. The complete database, including this DEM, is available as open-source in a web page dedicated to the international community of tsunami modellers (www.tsunarisque.cnrs.fr).

2. *Methods*

The database contains 300 measurements of tsunami height, flow depth, runup, and inundation distance. For these measurements, a variety of standard tsunami field survey techniques were combined (e.g., Tsuji *et al*., 1995; Okal *et al*., 2002), which has been previously published (Lavigne *et al*., 2006). Field data acquired using laser range finders (*LaserAce 300*) were calibrated from astronomical tide tables at Pulau Rusa and Uleelheue. The high density of field data allowed us to map the spatial distribution of tsunami height, flow depth, and runup, as well as the lines where the last transient tsunami bore collapsed several kilometers inland. At several sites, the highest marks on impacted trees or the upper limit of destruction traces on buildings decreased by several

meters in less than 100 m of distance, indicating a sudden energy loss attributed by the authors to collapse or "breaking" of a transient tsunami bore.

Flow directions for the tsunami waves, i.e., the angle with respect to the magnetic North, are evidenced by tilted trunks, pillars, and debris wrapped around trees. Two complementary methods were applied: (1) about 650 measures of flow orientation were collected using compass and GPS during two field surveys in January and August 2005; (2) About 400 additional data points (mostly coconut trunks in the rice fields) obtained through remote sensing and high-resolution air photograph as of June 2005 supplemented the database. For both methods, there is the potential for flow direction indicators to be biased due to the return flow. Therefore, landward flows and return flows were carefully distinguished in selecting only groups of parallel tilted trunks. This data set can be used to identify anomalous wave flow patterns such as interacting flows, and provide an additional means to evaluate the resolution of numerical simulations.

In order to complement these field data, interviews of eyewitnesses were conducted. Questionnaires were aimed at gaining a better understanding of the event's phenomenology. Information about the number of waves, the direction and timing of the flow, the location and shape of transient bores, and the sea retreat's distance was collected. However, forgetfulness, trauma, or influence of an official version of the event, may have influenced the testimonies given by local people, and the answers to our questionnaires were often approximate or even unreliable. For this reason, more reliable data to assess the arrival time of the tsunami waves were obtained through the analysis of three video recordings and the discovery of three broken clocks that stopped working when hit by a tsunami wave (see location in Fig. 1).

The patterns of building damage were investigated through the analysis of field survey, as well as aerial and satellite imagery. This technique compared existing buildings from before the tsunami to damage visible in post-event images. Over 6200 data points were collected and combined in a GIS framework using MapInfo® and Vertical Mapper® softwares, which allowed for a spatial representation of the building damage distribution. The damage level was classified based on structure vulnerability and level of damage (i.e., European Macro Seismic scale EMS98, Grunthal 1998, see Table 1).

3. Results

3.1. Earthquake Environmental Effects and Precursory Signs of Tsunami

In the Banda Aceh area, the great earthquake generated ground subsidence (MELTZNER *et al*., 2006), with amplitudes ranging from a few centimeters in Banda Aceh to about 2 meters along the west coast. Such large subsidence along the coast should have suggested to an aware observer the occurrence of a vertical displacement of the seafloor as a result of the earthquake, which was one natural warning signal of the incoming tsunami. In the

Table 1

Macro-tsunamic intensity scale based on buildings damages (from I to VI degrees). The term "Macro-tsunamic" is proposed by reference to the European Macro-Seismic intensity scale. This scale, developed by F. Leone, encompasses all building classes and damage levels

		Damage levels on buildings				
		D0 to D1	D1 to D2	D2 to D3	D4 to D5	D5 to D6
Buildings vulnerability classes	A	I	II	III	IV	V
	B	I	II	III	IV	VI
	C	II	III	IV	V	VI
	D	II	III	IV	V	VI
	E	II	IV	V	VI	VI

former swamp areas, transformed into shrimp basins or *tambak* along the north coast of Banda Aceh, liquefaction effects of clayed soils were observed. Eyewitnesses in Cotpaya or Miruk Taman (Fig. 2) described sulphurous, black water coming out of the ditches and sudden variations of well water levels, which were also mentioned by KITAGAWA *et al.* (2006). At Lampineung (Fig. 2), testimonies described malodorous black bubbles in water wells. Similar smells and colors were reported by fishermen roughly 1.5 km offshore. Along the karstic area of Lhok Nga, on the west coast, many wells were drained immediately following the earthquake.

Local people also reported hearing three detonations similar to bomb explosions that sounded between the main tectonic shock and the tsunami arrival. Similar noises were reported at the time of the 1933 Great Sanriku Earthquake in Japan (INOUYE, 1934) and of the 1977 Sumba earthquake and tsunami (KATO and TSUJI, 1995). These bangs are probably peculiar to earthquakes caused by the breaking of a sinking plate (KATO and TSUJI, 1995). However, SHUTO (1997) suggested that "thunder-like" sounds are generated and heard at distant places when tsunamis higher than 5 m hit coastal cliffs.

Another preliminary sign of the impending tsunami was a withdrawal of the ocean waters near the shore. The withdrawal related to the leading depression wave (SYNOLAKIS and TADEPALLI, 1996) was observed on the west coast about 10 minutes after the first shock of the earthquake. Testimonies reported similar observations at Meulaboh on the south coast (YALCINER *et al.*, 2005). The extent of the withdrawal exceeded 1 km off Banda Aceh and Lhok Nga, with the most reliable data being given by the Tuan Island, northwest off Uleelheue (Fig. 3). Located 1.2 km off the former coastline, the seawater surrounding this small island was drained during the leading depression wave related drawdown. The leading depression was estimated to 10 minutes. The corresponding lowering of the sea level has been estimated at 5 m $\pm$ 1 m by local fishermen. At Lampuuk (Fig. 4), the duration of the sea withdrawal lasted several minutes based on testimonies.

The last warning sign of the tsunami arrival was the massive migration of bird colonies flying landward from the open sea. Numerous eyewitnesses reported, after the disaster, to have heard bird calls which were interpreted by some villagers as a warning

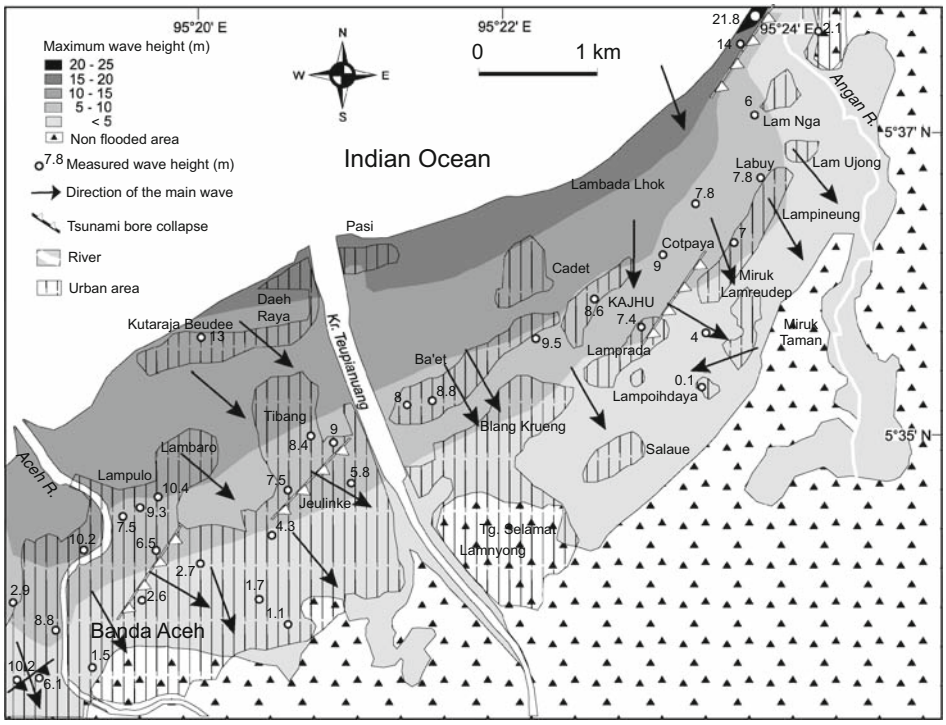

Figure 2
Tsunami propagation across the eastern part of the Banda Aceh plain.

for people threatened by the tsunami. This underlines the great efforts that still need to be focused on tsunami education and raising tsunami awareness.

3.2. Tsunami Waves and Velocities

Eyewitnesses reported between 10 and 12 waves along the coastlines all around the Banda Aceh area. The chief of the Fishery Regional Office at Uteuen Badeue (Fig. 1) recorded a dozen waves on videotape. Further west, eyewitnesses reported about ten waves from the bridge over the Teupianuang Canal, which was not inundated by the tsunami. Near downtown Banda Aceh, people who found shelter in the famous boat that overtopped a house at Lampulo also reported ten waves, like other eyewitnesses at Lampuuk and Labuhan (a military camp above the cement factory and the harbor: Fig. 4). However, several individual waves identified by the eyewitnesses may have resulted from the decomposition of single transient bores that have broken up into multiple waves.

Rather detailed descriptions were obtained for the first three waves. The leading wave moved rapidly landward as a turbulent flow with depths ranging from 0.5 to 2.5 m from

ground, depending on the local topography. The velocity of this flow was estimated to be approximately 8–10 $m.s^{-1}$, based on testimonies of some survivors at Lampuuk, who fled from this wave by motorcycle at a similar speed. The leading wave carried a large amount of debris. Several survivors reported that this wave was responsible for the destruction of most of the so-called *sederhana* and *semi-permanent* houses, as they are built using wood and bamboo. In spite of its limited depth and its solid waste, this flow moved as far as 2 km inland up to Ba'et village (Fig. 2), and as far as 3.5 km inland in downtown Banda Aceh. This first wave may have corresponded to the leading edge of the tsunami, i.e., the water that was being pushed by the second bore. Contrary to this leading wave, the second bore moved landward as a rapidly rising tide of dark color. Little is known about the following waves, which were lower than the subsequent waves, and thus came over areas already inundated and devastated. However, witnesses at Lampuuk, Uleelheue, Lamtengoh, northwest of Banda Aceh city, Figure 3, reported that the third wave was higher than the second one.

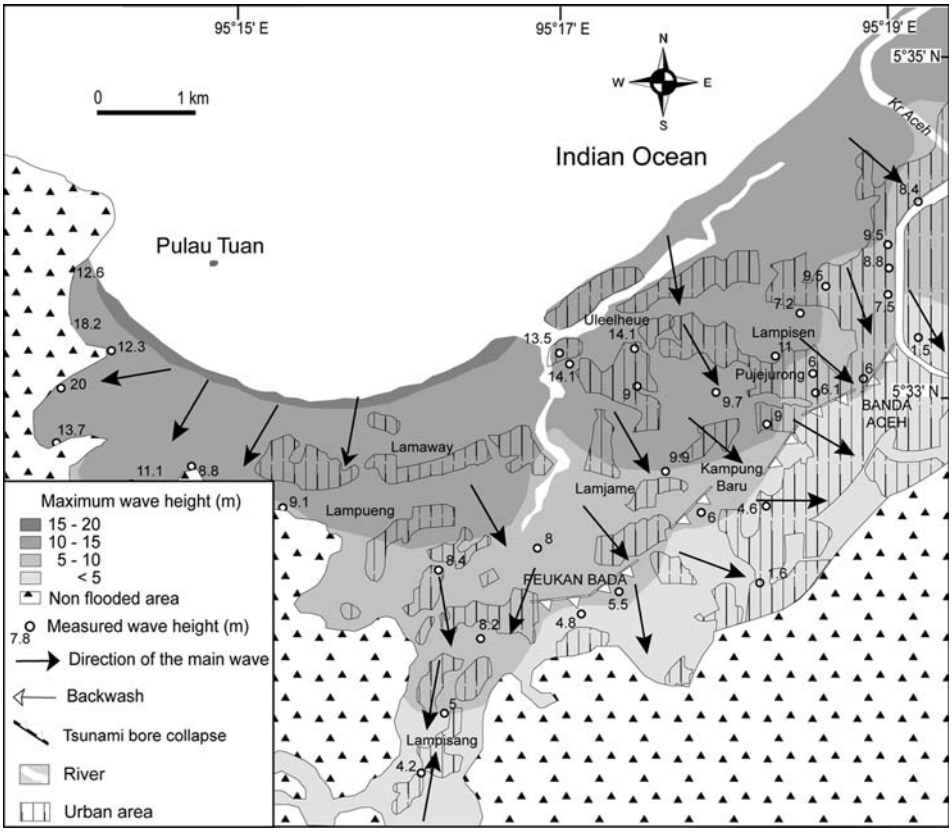

Figure 3
Tsunami propagation across the western part of the Banda Aceh plain.

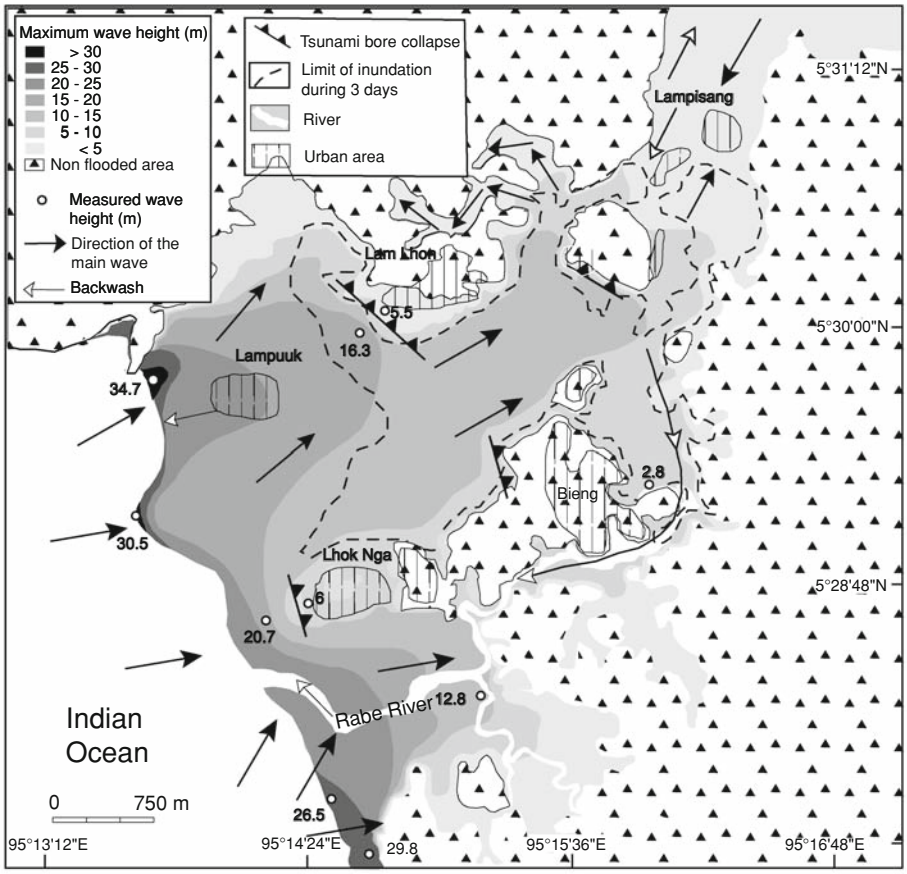

Figure 4
Tsunami propagation across the west coast (Lhok Nga subdistrict).

3.3. Tsunami Arrival Time

The tsunami arrival time is a fundamental parameter required to calibrate numerical models. However, accurate time data were difficult to obtain, due to contradictory testimonies and the scarcity of solid evidence that could be used to clarify the tsunami wave's chronology. Although also controversial, more accurate data based on stopped clocks and video sequences helped to estimate the tsunami velocity (Table 2).

On the west coast, the imam of Lhok Nga's main mosque heard people shouting "air laut naik" (the sea level raises) at 8:12 LT (t_{EQ} + 13 min), meaning that he heard the shouts when the sea started to return from its lowest receding level. The clock he found in his neighbor's house was broken by the leading wave at 8:20 LT (Fig. 5a) (t_{EQ} + 21 min). The second wave (the main one) occurred less than 5 minutes after the

Table 2

Characteristics of the tsunami waves on the 26 December 2004 in Banda Aceh District

		West coast		North coast			
		Lampuuk (mosque)	Lhok Nga (mosque)	Uleelheue (mosque)	Baiturrahman (mosque)	Lampulo (boat)	Teupianuang (bridge)
Coordinates (UTM)		747678 607764	748805 605982	753105 614607	756620 614340	757566 616755	760797 617865
Distance from coast (km)		0.7	1.3	0.1	2.5	1.5	2.2
Number of waves		~10	~10	> 3	2	~12	~10
Leading wave	Time	nd	8:20 LT (t_{EQ}+21 min)	nd	8:47 LT (t_{EQ}+48 min)	8:40 LT (t_{EQ}+41 min)	nd
	Direction (origin)	SW	SW	NW	NW	NW	NW
	Depth (m)	1.5	1	1.5	0.5	1	1
	Velocity ($m.s^{-1}$)	8-10	nd	very fast	1	nd	very fast
Second wave	Time	nd	8:25 LT (t_{EQ}+26 min)	nd	8:48 LT (t_{EQ}+49 min)	8:42/43 LT (t_{EQ}+43/44 min)	nd
	Direction	W	W	NW first, then NE & N	NW	NW first, then NE & N	NE first, then WNW & N
	Depth (m)	~20	8	~10	1.3	6	7 (Edge of the bridge)
	Velocity (m/s)	nd	nd	nd	4	nd	nd
Third wave	Time	nd	nd	nd		9:00 LT (t_{EQ}+61 min)	nd

LT: Local Time.
nd: no data.

Figure 5
Clocks stopped by the tsunami waves. A: Mr. Abu Abdul Rhaffar, Imam of Lhok Nga's main mosque, carrying a clock stopped by the first tsunami wave at 8:20 LT. B and C: Two clocks stopped by the second tsunami wave at Lampulo, 1.5 km from the open ocean. Located inside the same house near the boat, they stopped at 8:44 LT and 8:49 LT, respectively. (Photos: F. Lavigne).

first wave (t_{EQ} + 26 min) at Lampuuk and Lhok Nga, and no backwash was reported between these two waves at these locations. Although several testimonies reported the occurrence of a third wave higher than the second one, the exact chronology remains unclear.

At Lampulo, northeast of Banda Aceh (Fig. 1), a boat can still be found perched on the roof of a house 1.5 km from the ocean. The leading edge of the tsunami arrived along the north coast at approximately 8:40 LT. The second wave arrived 2 to 3 minutes after the leading wave (t_{EQ} + 42/43 min), and broke two clocks in a house (Fig. 5b). The first clock originally hung on a wall 2 m above the floor, stopped at 8:44 LT (t_{EQ} + 45 min), whereas the second one, hung at 3 m, stopped at 8:49 LT (t_{EQ} + 50 min). Considering a minimum flow velocity of 4 $m.s^{-1}$ calculated by Fritz *et al*. (2006) near the great mosque and at Peukan Bada, the front of the second wave reached the north coast less than 6 minutes before its arrival at the mosque (4 m/s × 1500 m), i.e. at t_{EQ} + 39 min or slightly less. The boat on the roof was carried by the third wave at about 9:00 LT (t_{EQ} + 61 min), i.e., about 10 minutes after the second wave. Eyewitnesses at Lampulo reported that the sea level withdrew by 1 m preceding the arrival of the third wave. This

small backwash between the second and the third wave was also observed in other locations, e.g., north of Cadet (Fig. 2).

At the Baiturrahman mosque in downtown Banda Aceh, the flow velocity of the leading wave did not exceed 1 $m.s^{-1}$ (Borrero, 2005b; Fritz *et al.*, 2006) due to the large amount of debris it was transporting. Based on a video frame analysis, the second tsunami wave arrived at the site only 40 seconds after its leading edge, with a flow velocity of 4 $m.s^{-1}$ (Fritz *et al.*, 2006). Assuming this velocity as constant from the shore to the mosque on a 2.5-km distance (whereas it was higher than this value), the second wave should have reached the city center in 10 minutes (4 $m.s^{-1}$ × 2500 m), i.e., at t_{EQ} + 49 min. This arrival time is twice the initial estimation of Borrero (2005b) who simply reported witness accounts during the immediate aftermath of the disaster. Such discrepancy underlines that the data obtained through broken clock and videos, although somewhat controversial, are still more reliable than information obtained by witnesses.

3.4. Flow Directions

Flow direction data obtained through eyewitness accounts and/or tilted trunks, pillars, and debris are of primary importance in reconstructing the wave's origin. Thus, a detailed analysis of the flow directions may help calibrate the numerical models.

The leading wave was almost perpendicular to the shore along the west coast, whereas it reached the northern shore from the northwest with an angle of 45° near the Aceh River mouth (Fig. 2) and Uleelheue (Fig. 3). The second wave reached Lhok Nga on the west coast from the southwest at an angle of about 45°. Therefore, its source may be attributed to the moment peak at about 4° N, rather than to the ones at 7° N and 9° N. This flow was moving as a single and massive tsunami front. On the northern coast, this front was divided into three segments of different directions, namely WNW, N and NE. On the eastern part of the Banda Aceh Bay, the northeast wavefront came first, whereas the northwest one came first at Uleelheue. These three segments of similar height (see below) probably resulted from the division of the second wave into separate waves after multiple refraction and diffraction effects near shore around the islands to the northwest of Banda Aceh (Fig. 1). In addition, some reflection effects may have enhanced the local effects of the tsunami, as also reported on Babi Island (Flores) in 1992 (Yeh *et al.*, 1994; Minoura *et al.*, 1997) and at Pangandaran (South Java) in July 2006 (Lavigne *et al.*, 2007). These waves collided with each other a few kilometers inland in several locations (e.g., at Jambutape, Lampulo, Lamprada, Lamjame: Fig. 2), as reported by testimonies or evidenced by trunks or pillars that were tilted in many different directions. The flow moving landward from Lhok Nga on the west coast interacted with the one moving from Uleelheue at Lampisang (Figs. 3 and 4). Such collision between waves may partly explain the differences in flow depth and orientations in neighboring areas.

3.5. Runup Heights

The apparent uniformity of the runup as indicated by the trim line (i.e., the upper limit of vegetation clearing by the tsunami on coastal hill slopes and cliffs) hundreds of kilometers along the west coast, typically 25 to 35 m, suggests that significant co-seismic submarine landslides were limited during the great Indian Ocean earthquake. Were this not the case, extreme runup values should have been locally identified (OKAL and SYNOLAKIS, 2003, 2004), as recently reported at Nusa Kambangan Island during the 17 July, 2006 tsunami that hit Java (FRITZ *et al*., 2007). A large mass failure capable of producing such a large wave has not been found yet for the 2004 tsunami event, even though marine surveys have taken place in search of such features along Sumatra's coast. Local geomorphological configurations of the coastline and/or the seafloor, however, were responsible for exceptional runup heights along the west coast of the Banda Aceh district. In Figure 6, the vegetation distribution along the cliff suggests that the runup heights varied from 27 m (left part of both pictures), which was the average tsunami height along the coast, to a maximum of 51 m (center of the picture). Even though this value is the highest recorded in human history for a non-landslide generated tsunami (cf. *NOAA National Geophysical Data Center*), this runup is roughly 10% of the 524 m runup marked by the trimline of the 1958 Lituya Bay landslide impact tsunami (MILLER 1960; FRITZ *et al*. 2001; FRITZ 2009, THIS ISSUE).

On the flat areas of the west coast, the tsunami height typically ranged from 25 to 35 m a.s.l., based on the height of the Filao trees near Lhok Nga's harbor. On the northeast coast, available data of tsunami heights are rather limited east of the Aceh

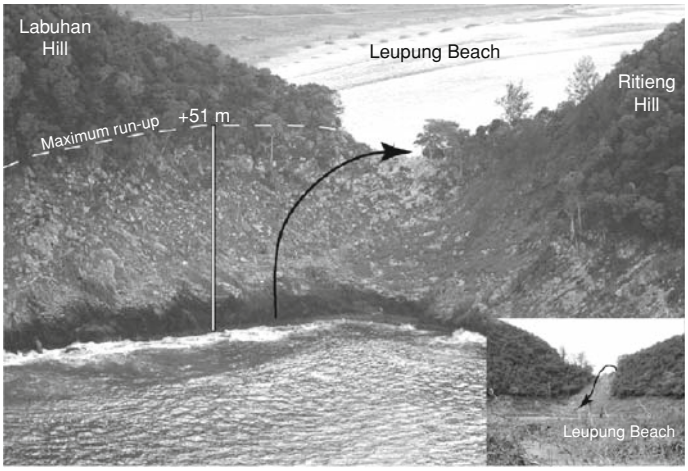

Figure 6
Runup height of 51 m a.s.l. measured on a cliff near Leupung, on the west coast (location in Fig. 1). The arrow displays the direction of the tsunami wave, which crossed the pass between Labuhan Hill and Ritieng Hill (Photos: F. Leone and F. Lavigne).

River, due to the lack of remaining trees and buildings. However, several reliable testimonies reported that the front of the second wave was as high as the coconut trees close to the shoreline, i.e., about 20 m a.s.l. On the eastern part of the bay, broken branches of Filao trees on sand dunes indicated runup values up to 22 m a.s.l. At Uleelheue, the maximum tsunami height did not exceed 13.5 m a.s.l. at the mosque.

3.6. Overland Tsunami Propagation

Landward motion of tsunamis is one of the lesser-known parameters for tsunami modeling. The rate that wave height and flow depth decrease with distance from the shoreline is poorly known, as are the factors that may explain the spatial variations of this rate. A recurrent question for the modellers is: Do the models require any additional basal friction to account for local topography, vegetation and buildings? Some results of our field investigations are presented below, which may help to answer this challenging question.

Before the collapse of the main tsunami bore two or three kilometers inland, the flow depth progressively decreased at a rate that ranged from 20 cm per 100 m to 60 cm per 100 m. At Lhok Nga on the west coast, this rate reached 50 cm per 100 m along the two first kilometers inland. Then was half this value across the 2-km long swamp further inland. On the coast north of Banda Aceh City, the flow depth decreased at various rates, i.e., 50 to 60 cm per 100 m on the eastern part of the bay (see Fig. 2), 25–30 cm per 100 m in the northeast suburbs of Banda Aceh City (e.g., at Lamparo or Jeulinke, Fig. 2), and 20 cm per 100 m on the northwest suburbs between Uleelheue and downtown Banda Aceh.

The above data may help define the role various factors play in controlling the rate at which flow depth decreases before the tsunami bore collapses.

The maximum rates were calculated at Lhok Nga and on the eastern part of the Banda Aceh Bay, where the maximum tsunami heights at the coastline were observed. Therefore the height of the main bore seems to play a key role in this rate, the higher the bore at the coastline, the higher the rate of decreasing flow depth. Indeed, the increase of flow depth due to a sudden increase of the nearshore slope (from 0.13% to 1.3% on the last 1.5 km) causes a drastic reduction of the tsunami velocity. This rapid dissipation of energy as the wave moves inland has also been inferred from the thickness, mean size, and sorting of the tsunami deposits in these areas (Paris *et al.*, 2007a; Jaffe *et al.*, 2006).

The local topography of the shore also played an important role in the landward reduction of flow depth. Indeed, huge sand dunes help to dissipate the wave's energy; at Lhok Nga and on the coast northeast of Banda Aceh, the dunes reaching elevations as high as 8 m a.s.l have been partly eroded by the tsunami. For an initial depth in excess of 20 m, the decreasing rate of the tsunami is about 50 cm per 100 m when the tsunami moves across a sand dune field. When the tsunami waves moved across swamps, shrimp basins or rice fields, the limited roughness of the ground explains lower decreasing rates, ranging around 20 cm per 100 m.

The role played by human settlements seems to be very limited before the collapse of the tsunami bore. Along the road between the Uleelheue mosque and downtown Banda Aceh, where the former traditional villages had previously been transformed into a residential area including concrete, two-story houses, the tsunami bore moved landward with a rather constant flow depth. The decreasing rate of flow depth was in the same order as the one calculated across non-built areas. Artificial dams and fringing reefs were also inefficient in locally reducing the tsunami velocity and depth (PARIS *et al*., 2007b).

3.7. Transient Tsunami Bores Formation and Collapse

For the first time since the major tsunamis crossed the Pacific in 1960 and 1964, the 26 December, 2004 event made it possible to accurately determine the location where the main tsunami bores collapsed due to the sudden energy dissipation of the second wave. Data based on field measurements (sudden decrease in flow depth) were always confirmed by relevant eyewitnesses, who used the Indonesian words "ombak pecah" (meaning "wave broke") to describe the collapse of the bores. Such data are of major importance when calibrating the numerical models that utilize this parameter. Thus far, the bore's collapse or "breaking" of tsunami waves has been analyzed mainly through physical modeling in artificial basins or through a mathematical approach (GRILLI *et al*., 1997). Our result will allow comparisons between these models and the 2004 field data.

Everywhere within the studied area, eyewitnesses described the shape of the propagating bore as similar to "standing cobra snake," meaning a high standing wave with vortex. Transient tsunami bores formed between 1.5 to 3 km inland (Figs. 3, 4, and 5). To the east of Banda Aceh Bay (Fig. 2), the bore related to the second wave collapsed in the rice fields south of the main road 1.7 km to 2 km from the coast line. In the northeast suburbs of Banda Aceh city, the propagating bore collapsed from 1.5 km, e.g., at Lamparo, to 3 km at Jeulinke, where the 7.5 m-high wave "broke" on the commercial buildings along the road. In the northwest suburbs of Banda Aceh City, the bore related to the second wave coming from Uleelheue collapsed near the Perusaahan Listrik Negara (PLN) boat, i.e., about 2.5 km inland from the open ocean. In this place, the flow depth suddenly diminished from 9–10 m to 1.5–2 m in a few hundred meters (Fig. 3).

The factors that contribute to the formation and disappearance of transient tsunami bores are difficult to assess. Some bores collapsed on contact with hill slopes. For example, Figure 5 shows a "breaking" line along the slope of a small hill covered with a coconut plantation, behind the golf course of Lhok Nga, located 1 km away from the shore. Due to the bore's collapse, the village was partially spared. Some survivors had taken refuge on the roofs of non-flooded houses. Another bore collapsed 2 km away from Lampuuk beach, at Lam Lhom village (Fig. 4). The flow depth suddenly decreased from about 16.5 m to 5.5 m over a distance of less than 100 m. Eyewitnesses described a "breaking wave" along a 5-m high palaeoshore covered by a coconut plantation that lies in front of the village. For the flat areas of the north coast, Figures 2 and 3 show that most

Figure 7 ▶

Investigation of tsunami-induced damage on building after the 26 December, 2004 tsunami. A. Studied area between Uleelheue and downtown Banda Aceh. B. Map of studied buildings. The selected area was divided in 25 ha squares. Within each square, the damaged building were precisely located using the freely available post-disaster high-resolution Quick Bird imagery (http://www.digitalglobe.com), and high resolution aerial photographs provided by Bakosurtanal (4970 units), from June 2005. C. Map of interpolated damage intensity for all building types (methodology and map conception: F. Leone).

of the bores collapsed where the flow depth ranges from five to ten meters. This may indicate a depth/velocity threshold for the destruction of the transient bores.

In addition with the local topographical settings, the collapse of the bores could have also been caused by the incoming flow interacting with the receding flow. However, the location of the interacting flows ("air beradu" in Indonesian language) reported by witnesses or enhanced through the flow direction map do not match with those of the bores' collapse. Furthermore, based on our field data, the density of human settlements did not play any role in the bore collapse process.

3.8. Flow Depth after Bores Collapses, Inundation Distance and Duration, and Backwash

Following the collapse of bores related to the second wave, the flow depth of the tsunami rapidly decreased. The runout flow spread over Banda Aceh City and its suburbs through foiled surges, sparing some districts and damaging others. The flow from Uleelheue encountered the one from Lampulo in the center of the city, where the flow depth did not exceed 2 m, based on the video recording analysis from Fritz *et al*. (2006). The high density of buildings explains why the flow was reduced within the city. To the east of the Aceh River, the presence of old beach ridges (or palaeoshores) running parallel to the current shore drastically reduced both flow depth and velocity of the second wave. The propagation of the following waves was stopped by the backwash of the second wave. Therefore, the inundation line did not exceed 2 km inland (Fig. 2). As for the tsunami wave coming from the west coast, it continued moving inland as far as 6 km, at which point it met the wave coming from the north coast.

On the north coast, the flow started to recede towards the ocean at about noon. At Kajhu (Fig. 2), the backwash lasted several hours during the first night following the disaster. The sea withdrawal was not regular, but occurred by steps. The mud lines at different levels, usually three, in the houses are evidence of periods of stagnant water that lasted for hours. At Lampulo, the flow depth was still 1 m at 14:30 LT, two and a half hours after the peak flow of 9 m. Therefore, the average velocity of the drawdown was about 5.3 cm per minute during this time interval. Closer to the shore, the current generated by the backwash was reported to be very fast. However, several indications suggest a laminar receding flow rather than a series of concentrated flows parallel to each other, including the absence of new gullies or other erosional features created by the backwash (Umitsu *et al*., 2007), the lack of sedimentary features of backwash within the tsunami deposits, as well as several testimonies. Contrarily, at Lampuuk (west coast),

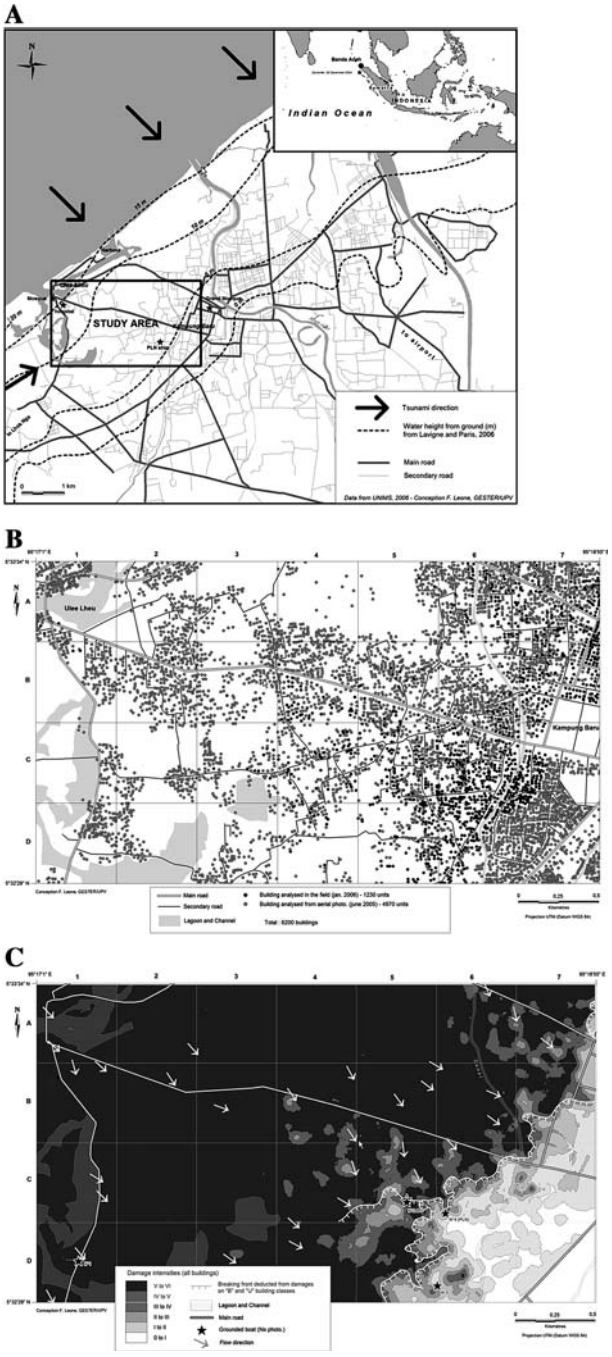
A
Indian Ocean
STUDY AREA
Tsunami direction
Water height from ground (m) from Lavigne and Paris, 2006
Main road
Secondary road
B
Ulee Lheu
Kampong Baru
Main road
Secondary road
Lagoon and Channel
Building analysed in the field (jan. 2006) - 1230 units
Building analysed from aerial photo. (june 2005) - 4970 units
Total : 6200 buildings
C
Damage intensities (all buildings)
Breaking front deducted from damages on "B" and "C" building classes
Lagoon and Channel
Main road
Grounded boat (No photo.)
Flow direction

the strong return current enlarged the river beds and created new gullies up to 20-m wide and 2-m deep (Paris *et al.*, 2007b).

The inundation lasted for three days at several sites. On the north coast, the long inundation preceding the backwash was mainly due to coseismic subsidence, which reached 0.50 m at Lampulo. The destruction of the polders by the tsunami, e.g., west to Uleelheue, may have favored the inundation. On the west coast, the tsunami flooded an approximate area of 65 km^2 between Lampuuk and Lampisang (Fig. 4). The inundation lasted three days, due to the combination of two factors. Firstly, what had once been a mangrove forest had previously been transformed into rice fields. Thus, this area is lower than the sandy shore, even after most of the sand dunes at Lampuuk were eroded by the tsunami. Therefore, the return flow followed the Rabe River instead of reversing and returning along the runup course. Secondly, a natural dam formed by tons of trees and debris of all types interrupted the backwash. A breach through the dam allowed the drainage of the stagnant water only three days after the tsunami event (Fig. 4).

3.9. Tsunami Intensity Based on Building Destruction

The integration and interpolation of 6200 damaged buildings in a GIS enabled reconstitution of the damage gradient in the northwestern suburbs of Banda Aceh city (Table 1 and Fig. 7). Nearly all of the buildings suffered grade 5 damage (i.e., destruction/collapse) and only a few reinforced-concrete buildings (e.g., a big mosque, the hospital, and a school at Uleelheue) suffered very heavy structural damage (grade 4). No substantial to heavy damage (grade 3) has been observed. Artificial embankments collapsed, and big boulders from these embankments or from the near-shore sea floor were moved inland (e.g., 85 tons of coral boulders in Labuhan: Paris *et al.*, 2007a). The tsunami also damaged port breakwaters, destroyed or washed away small vessels, and violently moved large vessels ashore. Figure 7c underlines a steep drop in the damage gradient around 2.7 km from the coast. Interestingly, four grounded boats are plotted exactly along the line of the bore's collapse, indicating a sudden drop in tsunami energy. This line was further refined using the Macro-tsunamic intensity scale (Table 1). The final shape of the line outlines digitations that can be associated with different wave heights or roughness variations of the topography. However, such lobes that are drawn on Figure 7 are difficult to interpret owing to the complex dynamics of the tsunami within the town.

4. Discussion and Conclusion

The 26 December, 2004 tsunami was an exceptional catastrophic event in the Banda Aceh area in every aspect.

The maximum tsunami height reached 35 m, i.e., approximately the height of a 10-story building, at the coastline of Lhok Nga, whereas historical records have rarely

exceeded 20 m. The maximum runup height reached 51 m on a high cliff at Labuhan. At least 3 factors may explain this record: (1) a "wave trap" morphology, i.e., a small bay oriented toward the wave train, (2) a 50° inclined cliff at the bay's upper two-thirds extent, and (3) a large continental shelf (25-km wide) with gentle slope gradient (0.13%).

The 26 December, 2004 tsunami caused the worst marine inundation ever reported in a large city located at more the 3 km from the shore. In almost every village, local eyewitnesses reported that the main tsunami waves were coming from two or three directions almost instantaneously. Trying to reconstruct the arrival time and flow direction of the main wave, which is supposed to have flattened most of the trees, was therefore quite challenging. Based on stopped clocks and video sequences, the front of the second wave reached the north coast about 40 minutes after the earthquake, i.e. twice the arrival time recorded on the west coast.

The tsunami's intensity in Indonesia ranked 6 (disastrous) on the Sieberg and Ambraseys' scale (AMBRASEYS, 1962), and XII (completely devastating) on the Papadopoulos and Imamura's scale (PAPADOPOULOS and IMAMURA, 2001). In both scales, it reached the highest intensity. Consequently, the tsunami is responsible for the deaths of more than 178,000 people in the Aceh province alone, including 90,000 in the city itself.

Many tsunami waves do not display any bore as they hit land, especially for slopes steeper than 12° (GRILLI *et al.*, 1997). They simply surge, flooding low-lying areas. During the Indian Ocean tsunami event, tsunami bores were observed as far as 3 km inland. At such distance, it can be assumed that the waves were "breaking" for the second or third time. However, field data display everywhere a progressive decreasing of the flow depth at a rate that ranged from 20 cm per 100 m to 60 cm per 100 m until the bore collapsed. Such data seem to act contradictorily with an assumption of transient bores reforming and "breaking" again.

The tsunami bore propagation plays a key role in the destruction processes of the buildings. Before crashing down on itself, the bore washed away all types of buildings except the huge mosques (e.g., at Lampuuk). The houses were totally destroyed independently of the flow depth when this depth exceeded 10 m. After the bore collapsed, water penetrated inland taking the form of fast-moving floods that have considerably less destruction power. Indeed, "postbreaking" behaviors exhibit a rapid

Table 3

Tsunami Intensity Scale proposed by PAPADOPOULOS and IMAMURA (2001) versus revised scale proposed by F. Leone in this paper

Intensity from Leone et al.	H(m)	Intensity from Papadopoulos et al., 2001
I	< 1.5	I to V
II	2	VI
III	3	VII to X
IV	5	
V	8	
VI	> 11	XI to XII

(nondissipative) decay associated with a transfer of potential energy into kinetic energy. Wave velocity decreases in this zone of rapid decay, as previously demonstrated by Grilli *et al*. (1997) through numerical modeling. Thus, the houses were damaged but not completely swept away after the bores' collapse. Our field observation on the aftermath of the July 2006 tsunami event in Java confirmed this affirmation. As the tsunami wave hit the Batukaras and the Permisan beaches of Java, the flow depth increased to over 10 meters (Lavigne *et al*., 2007). The houses close to the shore were completely destroyed, whereas houses were only slightly damaged beyond the line where the bore collapsed.

Our extensive field work made it possible to construct a tsunami damage intensity scale based upon quantitative data that includes all building classes and levels of damage. This scale is named here the "Macrotsunamic Intensity Scale" after the Macroseismic Intensity Scale of Grunthal (1998). Our results should also enhance the Tsunami Intensity Scale proposed by Papadopoulos and Imamura (2001; Table 3), which to date has not been calibrated for megatsunami events. In particular, the results of our comparison between damage gradients and flow depth suggest a need to revise the definition of the XI level of the Papadopoulos and Imamura (2001) scale, which is the "devastating" level associated with a tsunami height of > 16 m. Indeed, this scale indicates a damage of grade 5 in many masonry buildings, grade 4 in a few reinforced-concrete buildings, and grade 3 for most of the other reinforced-concrete buildings. On the north coast of Banda Aceh City (wave height around 16 m), most all of the buildings suffered grade 5 damage and only a few reinforced-concrete buildings suffered grade 4 damage. No grade 3 damage has been observed. Actually, 10 m seems to be the depth of water where the correlation between water depth and damage levels breaks down.

The open-source database obtained in the frame of the TSUNARISQUE programme offers an opportunity for worldwide researchers to better calibrate numerical models. Data includes high-resolution DEM of near-shore and coastal areas at Banda Aceh and Lhok Nga, tsunami and runup heights, flow depth, flow directions measured in the field, chronology of the waves, location of the hydraulic jumps, damage maps using a new quantitative-based tsunami intensity scale, and additional studies on sediment deposits previously published (Paris *et al*., 2006, 2007). Our field data will provide interesting challenges for mathematicians and earth scientists, including modeling of transient bore propagation and collapse, determining the friction and erosion processes of tsunami, modeling the turbulence, determining the effect of buildings and vegetation on the wave propagation, etc.

Acknowledgements

This paper is dedicated to the memory of our student and co-author Rino Cahyadi, who tragically died during a field trip in Thailand in 2007. The first measurements in January

2005 were achieved during the first ITST led by Prof. Tsuji. The following field surveys were carried out in the frame of the Tsunarisque Programme funded by the French Délégation Interministérielle pour l'Aide Post-Tsunami (DIPT), the French Embassy in Indonesia, and the French National Centre for Scientific Research (CNRS – ATIP Programme). The authors thank Waluyo, Syahnan, Laurent Mahieu and Nicolas Lespinasse, who contributed to field data acquisition, Marc Le Moullec and P.T. Enrique in Jakarta who provided high-resolution aerial photographs of the studied area. We also acknowledge the survivors of the disaster who have provided useful information about the event. We are also grateful to Chris Thissen for the correction of the English. J.-C. Borrero, K. Sieh, G. Greene, S. Bondevik, and an anonymous reviewer who provided thoughtful reviews of the early versions of the manuscript.

References

Ambraseys, N. N. (1962), *Data for the investigation of the seismic sea-waves in the Eastern Mediterranean*, Bull. Seismol. Soc. Am *52*, 895–913.

Ammon, C. J., Ji, C., Thio, H.-K., Robinsons, D., Ni, S., Hrorleifsdottir, V., Kanamori, H., Lay, T., Das, S., Helmberger, D., Ichinose, G., Polet, J., and Wald, D. (2005), *Rupture Process of the 2004 Sumatra-Andaman Earthquake*, Science *308*, 1133–1139.

Borrero, J.C. (2005a), *Field data and satellite imagery of the tsunami effects in Banda Aceh*, Science *308*, 1596.

Borrero, J.C. (2005b), *Field Survey of Northern Sumatra and Banda Aceh, Indonesia after the Tsunami and Earthquake of 26 December 2004*, Seismol. Res. Lett. *76*, 3, 312–320.

Borrero, J.C., Synolakis, C.E., and Fritz, H.M. (2006), *Field surveys of northern Sumatra after the tsunami and earthquake of 26 December 2004*, Earthq. Spectra *22*, S3, 93–104.

Carrier, G.F., Wu, T.T., and Yeh, H. (2003), *Tsunami runup and drawdown on a plane beach*, J. Fluid Mech. *475*, 79–99.

Chlieh, M., Avouac, J.-P., Hjorleifsdottir, V., Song, T.-R. A., Sieh, K., Sladen, A., Hébert, H. Prawirodirdjo, L., Bock, Y., and Galetzka, J. (2007), *Coseismic slip and afterslip of the great (Mw 9.15) Sumatra–Andaman Earthquake of 2004*, Bull. Seismol. Soc. Am *97*, 152–173.

Engdahl, E.R., Villaseñor, A., DeShon, H.R., and Thurber, C.H. (2007), *Teleseismic relocation and assessment of seismicity (1918–2005) in the region of the 2004 M_w 9.0 Sumatra–Andaman and 2005 Mw 8.6 Nias Island great earthquakes*, Bull. Seismol. Soc. Am. *97*, 1A, S43–S61.

Fritz, H., M., Kongko, W., Moore, A., McAdoo, B., Goff, J., Harbitz, C., Uslu, B., Kalligeris, N., Suteja, D., Kalsum, K., Titov, V., Gusman, A., Latief, H., Santoso, E., Sujoko, S., Djulkarnaen, D., Sunendar, H., and Synolakis, C. (2007), *Extreme runup from the 17 July 2006 Java tsunami*, Geophys. Res. Lett. *34*, L12602.

Fritz, H.M., Borrero, J.C., Synolakis, C.E., and Yoo, J. (2006), *2004 Indian Ocean tsunami flow velocity measurements from survivor videos*, Geophys. Res. Lett. *33*, L24605.

Fritz, H.M., Hager, W.H., and Minor, H.E. (2001), *Lituya Bay case: Rockslide impact and wave run-up*, Science of Tsunami Hazards *19*, 3–22.

Fritz, H.M., Mohammed Fi, and Yoo, Y. (2009), *Lituya Bay Landside Impact Generated Mega-Tsunami: 50th Anniversary*, Pure. Appl. Geophys. *166,* 1/2 (2009), this issue

Fu, G. and Sun, W. (2006), *Global co-seismic displacements caused by the 2004 Sumatra-Andaman earthquake (M_w 9.1)*, Earth Planets Space *58*, 149–152.

Geist, E.L., Titov, V.V., Arcas, D, Pollitz, F.F., and Bilek S. L. (2007), *Implications of the 26 December 2004 Sumatra–Andaman earthquake on tsunami forecast and assessment models for great subduction-zone earthquakes*, Bull. Seismol. Soc. Am. *97*, 1A, S249–S270.

Grilli, S.T., Svendsen, I.A., and Subramanya, R. (1997), *Breaking criterion and characteristics for solitary waves on slopes*, J. Waterway Port Coastal and Ocean Engineering *123*, 3, 102–112.

GOTO, C., OGAWA, Y., SHUTO, N., and IMAMURA, N., *Numerical method of tsunami simulation with the leap-frog scheme* (IUGG/IOC Time Project) (IOC Manual, UNESCO, New York 1997)

HÉBERT, H., HEINRICH, P, SCHINDELÉ, F., and PIATANESI, A. (2001), *Far-field simulation of tsunami propagation in the Pacific Ocean: Impact on the Marquesas Islands (French Polynesia)*, J. Geophys. Res. *106*, C5, 9161–9177.

HÉBERT. H., SLADEN A., and SCHINDELÉ, F. (2007), *Numerical Modeling of the Great 2004 Indian Ocean Tsunami: Focus on the Mascarene Islands*, Bull. Seismol. Soc. Am. *97*, 1A, S208–S222.

HEINRICH, P., SCHINDELÉ, F., GUIBOURG, S., and IHMLÉ, P.F. (1998), *Modeling of the February 1996 Peruvian tsunami*, Geophys. Res. Lett. *25*, 2687–2690.

IMAMURA, F., and SHUTO, N., *Tsunami propagation by use of numerical dispersion*. In *Proceedings, International Symposium Comp. Fluid Dynamics* (Nagoya, 1990) pp. 390–395.

INOUYE, W. (1934), *On sound phenomena of the Sanriku earthquake of March 3rd, 1933*, Bull. Earthq. Res. Instit. Extra *1*, 77–86 (in Japanese).

JAFFE, B.E., BORRERO, J.-C., PRASETYA, G.S., PETERS, R., MCADOO, B., GELFENBAUM, G., MORTON, R., RUGGIERO, P., HIGMAN, B., DENGLER, L., HIDAYAT, R., KINGSLEY, E., KONGKO W., LUKIJANTO, and MOORE A. (2006), *Northwest Sumatra and Offshore Islands field survey after the December 2004 Indian Ocean Tsunami*. Earthquake Spectra *22*, S3, S105-S135.

KATO, K. and TSUJI, Y. (1995), *Tsunami of the Sumba earthquake of August 19, 1977*, J. Natural Disaster Sci. *17*, 2, 87–100.

KIRBY, J.T. (2003), *Boussinesq models and applications to nearshore wave propagation, surf-zone processes and wave-induced currents*. In Lakhan V.C., ed., *Advances in Coastal Engineering*, (Elsevier, 2003) pp. 1–41.

KITAGAWA, M., KOIZUMI, Y., TAKAHASHI, M., MATSUMOTO, N., and SATO, T. (2006), *Changes in groundwater levels or pressures associated with the 2004 Earthquake off the west coast of northern Sumatra (M9.0)*, Earth Planets Space *58*, 173–179.

LAVIGNE, F., PARIS, R., WASSMER, P., GOMEZ, C., BRUNSTEIN, D., GRANCHER, D., VAUTIER, F., SARTOHADI, J., SETIAWAN, A., SYAHNAN, GUNAWAN, T., FACHRIZAL, WALUYO, B., MARDIATNO, D., WIDAGDO, A., CAHYADI, R., LESPINASSE, N., and MAHIEU, L. (2006), *Learning from a major disaster (Banda Aceh, December 26th, 2004): A methodology to calibrate simulation codes for tsunami inundation models*, Zeitschrift für Geomorphologie N.F., Suppl. *146*, 253–265.

LAVIGNE, F., GOMEZ, C., GIFFO, M., WASSMER, P., HOEBRECK, C., MARDIATNO, D., PRIOYONO, J., and PARIS, R. (2007), *Field observations of the 17th July 2006 Tsunami in Java*, Nat. Hazard and Earth Sci. Syst. *7*, 177–183.

LAY, T., KANAMORI, H., AMMON, C.J., NETTLES, M., WARD, S.N., ASTER, R.C., BECK, S.L., BILEK, S.L., BRUDZINSKI, M.R., BUTLER, R., DESHON, H.R., EKSTRÖM, G., SAKATE, K., and SIPKIN, S. (2005), *The great Sumatra-Andaman earthquake of 26 December 2004*, Science *308*, 1127–1133.

MELTZNER, A.J., SIEH, K., ABRAMS, M., AGNEW, D.-C., HUDNUT, K.-W., AVOUAC, J.-P., and NATAWIDJAJA, D. H. (2006), *Uplift and subsidence associated with the great Aceh-Andaman earthquake of 2004*, J. Geophys. Res. *111*, B02407, doi:10, 1029/2005JB003891.

MILLER, D.J. (1960), *Giant waves in Lituya Bay*, Alaska. U.S. Geological Survey Professional Paper 354C, 51–83.

MINOURA, K., IMAMURA, F., TAKAHASHI, T., and SHUTO, N. (1997), *Sequence of sedimentation processes caused by the 1992 Flores tsunami: Evidence from Babi Island*, Geology *25*, 6, 523–526.

OKAL, E.A., and SYNOLAKIS, C.E. (2003), *Theoretical comparison of tsunamis from dislocations and landslides*, Pure Appl. Geophys. *160*, 2177–2188.

OKAL, E.A., and SYNOLAKIS, C.E. (2004), *Source discriminants for near-field tsunamis*, Geophysical Journal International *158*, 899–912.

OKAL, E A., DENGLER, L., ARAYA, S., BORRERO, J.C., GOMER, B., KOSHIMURA, S., LAOS, G., OLCESE, D., ORTIZ, M., SWENSSON, M., TITOV, V.V., and VEGAS, F. (2002), *A field survey of the Camana, Peru tsunami of June 23, 2001*, Seismol. Res. Lett. *73*, 904–917.

PAPADOPOULOS, G.A. and IMAMURA, F., *A proposal for a new tsunami intensity scale.* In *Proc. Internat. Tsunami Conf.* 7–9 August 2001 (Seattle 2001) pp. 569 - 577.

PARIS, R., LAVIGNE, F., WASSMER, P., and SARTOHADI, J. (2007a), *Coastal sedimentation associated with the December 26, 2004 tsunami in Lhok Nga, West Banda Aceh (Sumatra, Indonesia)*, Marine Geology *238*, 93–106.

PARIS, R., WASSMER, P., SARTOHADI, J., LAVIGNE, F., BARTHOMEUF, B., DESGAGES, E., GRANCHER, D., BAUMER, P., VAUTIER, F., BRUNSTEIN, D., and GOMEZ, C. (2007b), *Tsunamis as geomorphic crisis: Lessons from the December 26, 2004 tsunami in Lhok Nga, West Banda Aceh (Sumatra, Indonesia)*, Geomorphology (in press).

SHUTO, N., *A natural warning of tsunami arrival*. In *Perspectives on Tsunami Hazard Reduction, Observation Theory and Planning, Advances in Natural and Technological Hazards Research* (ed. Hebenstreit G. T.) (Springer, 1997) pp. 157–173.

STEIN, S. and OKAL, E. (2005), *Speed and size of the Sumatra earthquake*, Nature *434*, 581–582.

SYNOLAKIS, C.E. (1987), *The runup of solitary waves*, J. Fluid Mech. *185*, 523–545.

SYNOLAKIS, C.E., OKAL, E.A., and BERNARD, E.N. (2005), *The Megatsunami of December 26 2004*, The Bridge *35*, 2, 26–35.

TADEPALLI, S. and SYNOLAKIS, C.E. (1996), *Model for the leading waves of tsunamis*, Phys. Rev. Lett. *77*, 2141–2145.

TITOV, V.V., and SYNOLAKIS, C.E. (1998), *Numerical modeling of tidal wave runup*, J. Waterways, Port, Coastal and Ocean Engin., ASCE *124*, 4, 157–171.

TITOV, V.V., ARCAS, D., KANOGLU, U., NEWMAN, J., and GONZALEZ, F.I. (2004), *Inundation modeling for probabilistic tsunami hazard assessment*, EOS Trans. AGU *85*, 47, Fall Meeting Suppl., Abstract OS23D–1340.

TSUJI, Y., IMAMURA, H., MATSUTOMI, H., SYNOLAKIS, C.E., NANANG, P.T., JUMADI, HARADA, S., HAN, S.S, ARAI, K., and COOK, B. (1995), Field survey of the east Java earthquake and tsunami of June 3, 1994, Pure Appl. Geophys. *144*, 3–4, 839–854.

TSUJI, Y., TANIOKA, Y., MATSUTOMI, H., NISHIMURA, Y., KAMATAKI, T., MURAKAMI, Y., SAKAKIYAMA, T., MOORE, A., GELFENBAUM, G., NUGROHO, S., WALUYO, B., SUKANTA, I., TRIYONO, R., and NAMEGAYA, Y. (2006), *Damage and height distribution of Sumatra earthquake-tsunami of December 26, 2004, in Banda Aceh City and its environs*, J. Disaster Res. *1*, 1, 103–115.

UMITSU, M., TANAVUD, C., and PATANAKANOG, T. (2007), *Effects of Landforms on Tsunami Flow in the Plains of Banda Aceh, Indonesia, and Nam Khem*, Thailand, Marine Geology (in press).

VALLÉE, M. (2007), *Rupture properties of the giant Sumatra earthquake imaged by empirical Green's function analysis*, Bull. Seismol. Soc. Am. *97*, S103–S114.

WONG, F.L., GEIST, E.L., and VENTURATO, A., J., *Probabilistic Tsunami Hazard Maps and GIS*. In Proc. 2005 ESRI Internat. User Conf., (San Diego California, July 2005), 11 pp.

YALCINER, A.C., PERINCEK, D., ERSOY, S., PRESATEYA, G.S., HIDAYAT, R., and MCADOO, B. (2005), *December 26, 2004 Indian Ocean Tsunami field survey (Jan. 21–31, 2005) at north of Sumatra Island*, http://yalciner.ce.metu.edu.tr/sumatra/survey/

YEH, H., LIU, P.L.F., BRIGGS, M., and SYNOLAKIS, C.E., (1994), *Tsunami catastrophe in Babi Island*, Nature, *372*, 6503–6508.

(Received January 20, 2001, accepted September 17, 2008)
Published Online First: February 13, 2009